Spatial effects of radiation trapping in an optically thick atomic vapor excited by a laser beam

T. Scholz, M. Schiffer, J. Welzel, D. Cysarz, and W. Lange
Institut für Angewandte Physik, Westfälische Wilhelms-Universität Münster, Corrensstraße 2/4, D-48149 Münster, Germany
(Received 5 July 1995)

We describe the influence of radiation trapping on the spatial distribution of the excited-state population in sodium vapor, interacting with a linearly polarized Gaussian laser beam. Counterintuitively the excitation volume experiences a strong spatial shrinking at high optical depth. The interpretation of this nonlocal effect is based on the numerical solution of the stationary Holstein equation, which takes into account the full frequency dependence of the reabsorption probability within the process of diffusion of radiation. The calculations performed are in good qualitative agreement with the spatial effects observed experimentally.

PACS number(s): 32.80.−t, 32.70.Jz, 32.50.+d

A laser beam passing through a cell filled with a resonant two-level atomic medium will populate the excited state of the atoms. In a direction perpendicular to the exciting laser beam, fluorescence light generated by spontaneous emission indicates the spatial distribution of the excited-state population. In a medium of low optical depth, fluorescence will be emitted only from a spatial region limited by the laser beam volume. If the optical depth is increased, the process of diffusion of radiation [1] comes into play and a part of the spontaneously emitted resonance radiation is then likely to be reabsorbed outside the region excited by the laser beam, thus transferring excitation to the surrounding volume. Consequently the volume of the excitation should increase and fluorescence light should be emitted even from regions far outside of the laser beam. The surprising observation, however, is the following: We find a dramatic shrinking of the diameter of the fluorescent region, when the optical depth is further increased. Though this phenomenon must have been observed before, we are not aware of any analysis. In this paper we are going to show that this effect is a consequence of the multiple scattering of resonance fluorescence and represents a spatial effect generic in the process of diffusion of radiation. Spatial distributions of atomic variables, however, are often of substantial interest in many experimental situations. Especially in the field of nonlinear optics the spatial distribution of these variables is essential and may be influenced by diffusion of radiation. This has, e.g., been shown in theoretical [2,3] and experimental studies that were focused on the spatial and temporal influence of radiation trapping on the population of sublevels of the atomic ground state [4–6]. In this paper, however, we will report on a complementary experimental situation concerning the peculiar behavior of the spatial distribution of the population of the excited atomic state.

In our studies we use the experimental setup illustrated in Fig. 1. Sodium vapor is contained in a cylindrical glass cell of 2 cm diameter. The length of the interaction zone is 3 cm. Measurements are performed under a buffer gas pressure of 20 and 200 hPa of argon. The sodium resistant glass cell can be used for temperatures up to 420 °C, but the observations are restricted to a temperature regime from 160 to 340 °C. At these temperatures the particle densities vary between 2.8×10^{11} and 4.4×10^{14} cm^{-3} and the optical depth lies in a range from $k_0R=10^{-1}$ to 10^3, where k_0 is the line center absorption coefficient and R the cell radius. The particle densities are determined with the help of the linear Faraday effect [7], with an uncertainty of the absolute value of 20%. A cw ring dye laser tuned near to the sodium D_1 line, provides a power of up to 150 mW, measured at the cell entrance. The Gaussian laser beam (TEM_{00}) is spatially filtered and has a $1/e^2$ radius of 0.5 mm in the interaction region. The transmission of the laser beam is adjusted to (85 ± 5)% by varying the detuning between 0 and 140 GHz, so that effects due to pump wave depletion are negligible. A measure for the strength of the coupling of the laser excited volume to the surrounding medium is simply the spatial distribution of excited atoms inside the cell volume, indicated by the fluorescence emitted in the plane transverse to the laser beam. The width of these profiles represents a measure for the penetration depth of the resonance fluorescence into the medium. Using a charge-coupled device (CCD) camera and an image processing system, the spatial distribution of the fluorescence intensity is measured as indicated in Fig. 1 for a wide range of particle densities. This quantity gives an upper limit for the spatial distribution of the excited-state density (cf. Ref. [8]).

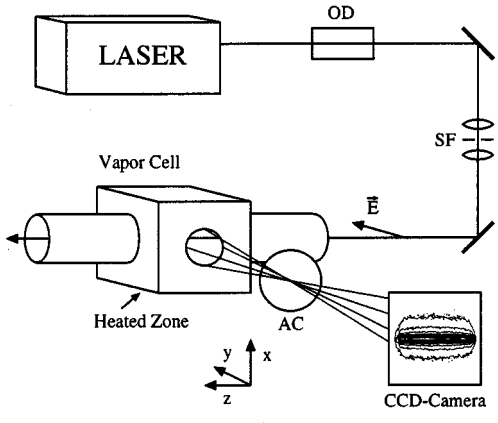

FIG. 1. Schematic of the experimental setup. OD: optical diode; SF: spatial filter; AC: achromat. Typical spatial distribution (contour) of the fluorescence shown on the CCD camera for $T=220$ °C and $p=200$ hPa argon.

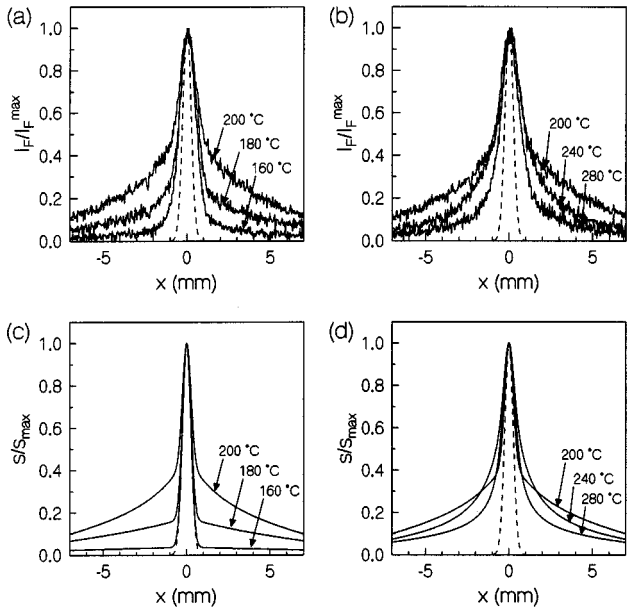

FIG. 2. (a), (b): measured steady-state profiles of the laser induced fluorescence transverse to the laser direction (cut through the CCD camera image) at 20 hPa argon. (c), (d): calculated profiles of $s(x)$ due to Eqs. (1) and (2) at 20 hPa argon ($P_0 = 0.12$ MHz $\ll \Gamma_1 = 61.2$ MHz). The densities for the numerical calculations have to be taken from the experimental data. Dashed lines: laser profile ($w = 0.5$ mm).

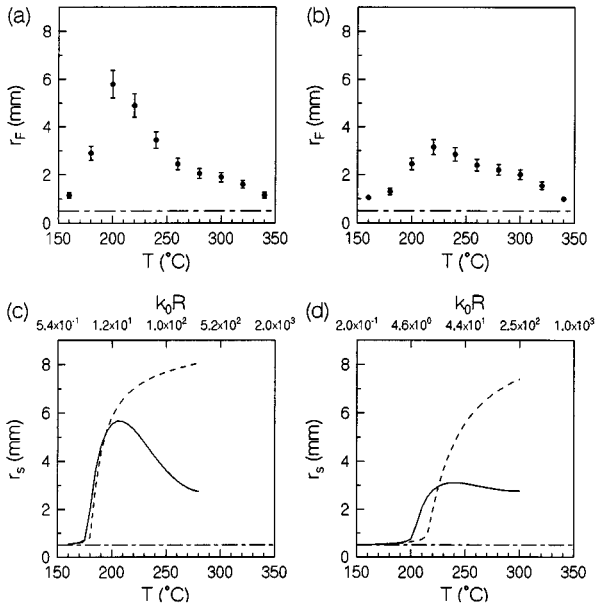

FIG. 3. Measured $1/e^2$ radii of the spatial fluorescence distributions for various temperatures of the heated cell at 20 hPa (a) and 200 hPa (b) pressure of argon buffer gas. Calculated $1/e^2$ radii for $s(x)$ [mean free path model: dashed line (cf. Refs. [8,16,17])] and from Eqs. (1) and (2) (solid line) at 20 hPa (c) and 200 hPa (d) argon (same parameters as in Fig. 2). Laser beam radius $w = 0.5$ mm (dashed-dotted line). The optical depth includes the measured sodium density.

Typical results of these experiments are shown in Figs. 2(a) and 2(b), where a cut through the CCD camera image transverse to the direction of the laser beam (x direction in Fig. 1) is depicted. At first the transverse profiles are considerably increasing in width with increasing particle density up to a maximum of about 12 laser beam diameters at 20 hPa argon and 6 laser beam diameters at 200 hPa argon [cf. Figs. 3(a) and 3(b)]. Surprisingly the diameter decreases again at higher densities. We also measure the fluorescence intensity spatially integrated over the entire CCD chip area (cf. Fig. 4), which is a measure of the energy flux of the fluorescence light emerging from the cell. Figure 4 shows that this energy flux can be kept constant up to 300 °C, whereas the shrinking of the spatial profiles of the fluorescence starts at 220 °C at 20 hPa and 240 °C at 200 hPa argon, respectively. At 320 and 340 °C a significant part of the fluorescence energy is lost (cf. Fig. 4) due to the fact that the dimer concentration and the trapping times are growing simultaneously, so that nonradiative quenching [9] becomes increasingly significant. To exclude that the spatial shrinking up to 300 °C is due to excitation transfer to sodium dimers [9] one has to compare the rate coefficient of energy transfer Γ_q [10] and the effective decay rate $\Gamma_{\text{eff}} = g\Gamma_1$ [11], where the average number of reabsorptions is given by $1/g$ and the decay rate for spontaneous emission is denoted Γ_1. At 280–300 °C and a measured sodium density of about 10^{14} cm^{-3} the vapor typically contains a fraction of about 1% of Na_2 [9], yielding $\Gamma_q/\Gamma_{\text{eff}} = 3\%$ at 280 °C for a purely Doppler broadened line and 0.2% at 300 °C and 200 hPa for a purely pressure broadened line [10,11], hence effects due to dimer quenching should play a minor role below 300 °C.

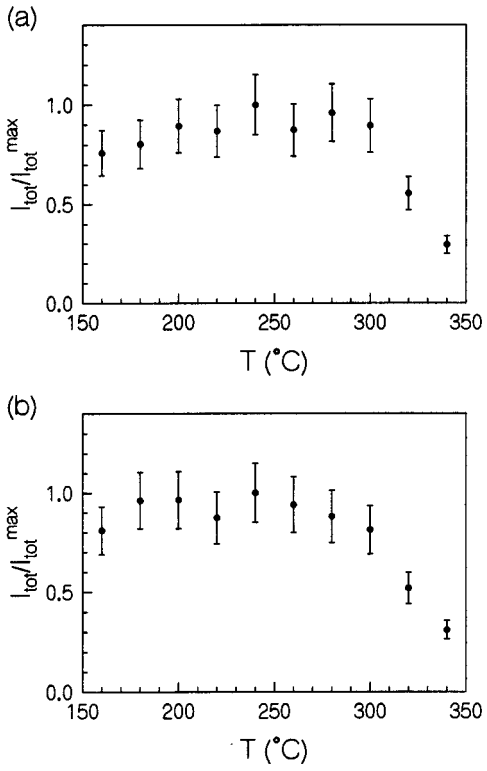

FIG. 4. Normalized spatially integrated fluorescence intensity at 20 hPa (a) and 200 hPa (b) argon buffer gas pressure.

Most theoretical treatments concerning the process of diffusion of radiation have been based on a formulation using the Holstein equation [1]. This equations allows a spatial-temporal calculation of the excited atomic state under conditions of radiation trapping. With the assumption of complete redistribution [12] the stationary integral equation reads in an one-dimensional formulation:

$$\Gamma_1 s(x) = P(x) + \Gamma_1 \int_{-R}^{+R} dx' G(x,x') s(x'), \tag{1}$$

$$G(x,x') = \frac{1}{2} \int_{-\infty}^{+\infty} d\nu \kappa \phi^2(\nu) \exp\{-\kappa \phi(\nu) |x - x'|\}. \tag{2}$$

Here s represents the population of the excited state in a two-level medium, x is the coordinate transverse to the laser beam (cf. Fig. 1), and R the cell radius. $P(x) = P_0 \exp\{-2(x/w)^2\}$ is the pump rate for the Gaussian laser beam centered at $x=0$ with $1/e^2$ radius w. The absorption coefficient is given by $k(\nu) = \kappa \phi(\nu)$ with the normalized line-shape function $\phi(\nu)$ [$\int_{-\infty}^{+\infty} d\nu \phi(\nu) = 1$] defined by [13]

$$\phi(\nu) = \sqrt{\frac{\ln 2}{\pi}} \frac{1}{\Gamma_D} u(\tilde{\nu}, a). \tag{3}$$

$\tilde{\nu} = \sqrt{\ln 2}(\nu - \nu_0)/\Gamma_D$ is a normalized frequency where ν_0 is the resonance frequency of the sodium D_1 line. The Voigt parameter $a = \sqrt{\ln 2}\Gamma_L/\Gamma_D$ includes Γ_L and Γ_D, the collision and Doppler broadening widths and u is the real part of the complex Voigt function (cf. Ref. [13] and references therein). $\kappa = \lambda^2 N \Gamma_1/(8\pi)$ is proportional to the absorption coefficient k_0 in line center. Furthermore it is assumed that no saturation ($P_0 \ll \Gamma_1$) and no quenching ($\Gamma_q \ll \Gamma_{\text{eff}}$) occurs.

Analytical solutions of the Holstein integral equation have been found for several special situations, e.g., the infinite slab and infinite cylinder geometries (cf. Refs. [14,15] and references therein). Asymptotic expansions for $s(x)$ have been calculated in the regime of high optical depth ($k_0 R > 10$) for different line shapes [14] and the spatial profile in the fundamental mode [1] has been discussed in more detail for the case of an infinitely long cylinder [15]. Very recently new analytical models have also been developed for the solution of the Holstein equation at low optical depth ($k_0 R < 5$) [8,16,17]. In this situation a single photon mean free path can be defined and the Holstein equation can be transformed to a Milne-type diffusion equation [17,18].

Concerning the spatial effects of diffusion of radiation one intuitively would expect that in a gaseous medium excited by a resonant Gaussian laser beam the stationary $1/e^2$ width of the resulting transverse excited-state profiles should increase constantly with growing particle density. As can be seen from the experimental curves in Figs. 2 and 3, this is in contradiction to the observation. This is mainly due to the fact that in every emission process there is a certain probability for the photons to be emitted in the far wings of the resonance line. These photons are then likely to escape the cell volume without further scattering, thus introducing a certain loss to the process of radiation trapping. A well-known consequence of this effect is the self-reversed spectral distribution of the fluorescence intensity emerging from the cell at higher optical depths [14].

In order to gain a better understanding we first consider a simplified version of the radiation transport process. Let us assume that different classes of photons can be emitted, which represent limiting cases: resonant photons, which are reabsorbed within a mean free path, and off-resonant ones, which immediately leave the cell geometry without further reabsorption. The resonant contribution can be described by a Milne-type diffusion equation [18], with a mean free path decreasing with increasing sodium density of course. On the other hand, there is a probability for the emission of off-resonant photons, causing a certain loss in every reemission process. In any case, for small densities almost no radiation trapping occurs. Thus, at a certain position x_0 outside the laser beam volume, the population of the excited state s is small. At higher densities radiation trapping starts to become important and $s(x_0)$ increases. Finally, with further increased sodium density, the mean free path for resonant photons is drastically reduced and the number of reabsorptions it takes the excitation energy to reach x_0 is growing. After many reemissions, each accompanied by the loss due to the emission into the off resonant frequency component, the population of the excited state has then already decreased significantly when it finally reaches x_0.

Although this is an oversimplified intuitive explanation, the interpretation remains valid in our theoretical treatment. Since the experiment covers a regime of low, moderate, and high optical depth (cf. Ref. [19]) and no closed analytical solution of the Holstein equation is available throughout the entire regime of optical depths we solve Eqs. (1) and (2) numerically. We performed extensive calculations on a RISC workstation system using a set of 185 frequencies to represent a Voigt emission and absorption line shape with $a = 0.16$ ($a = 1.6$) at 20 hPa (200 hPa) and 160 °C, slightly decreasing with temperature [cf. Eq. (3)]. The stationary integral equation (1) is evaluated on a grid in real space (cf. Ref. [20]) with up to 4000 mesh points. The resultant set of linear algebraic equations is then solved by standard techniques. Numerical solutions of $s(x)$ are presented in Figs. 2(c) and 2(d). Figures 3(c) and 3(d) show the theoretical curves of the $1/e^2$ radius of the transverse excitation profiles with increasing temperature and optical depth. As can be seen, the characteristic behavior of the spatial shrinking of the curves obtained experimentally is reproduced very well. Though self-reversal is enhanced by line broadening the spatial shrinking at higher particle density is less marked [cf. Fig. 3(d), solid line] due to the fact that the line center absorption coefficient decreases at higher buffer gas pressure. If Eq. (1) is normalized onto the cell radius it only depends on the optical depth and the line profile and so the shrinking is mainly an optical depth phenomenon. Although it is a well-known fact that the mean free path approximation [8,16,17] fails at higher optical depth [14,15,17,19], we finally compare our numerical results with this model [cf. Figs. 3(c) and 3(d)], in order to demonstrate the drastic deviation of the radiation trapping process from a purely diffusive behavior.

In conclusion it has to be emphasized that the complex spatial behavior of the process of diffusion of radiation experimentally observed can be interpreted with the help of the

well-known Holstein integral equation [1], which adds nonlocality to the optical properties of the system. The Holstein equation includes a certain loss mechanism due to the frequency dependence of the reabsorption probability. Even without quenching it is this loss that is responsible for the observed shrinking of the excited-state profiles, when at higher optical depth self-reversal becomes important. Under these experimental conditions the spatial properties of the radiation trapping process are of considerable importance in the interpretation of nonlinear optical experiments such as self-focusing and defocusing as well as conical emission. Investigations on these topics, especially under conditions of saturation of the atomic resonance, are currently under way. We suppose that the influence of the described effect may play its role for experiments in traps with high particle densities [21] and we suggest that the spatial effects of radiation trapping should be taken into account in the discussion of schemes proposed for recoil lasers [22].

[1] T. Holstein, Phys. Rev. **72**, 1212 (1947).
[2] A. W. McCord, R. J. Ballagh, and J. Cooper, Opt. Commun. **68**, 375 (1988).
[3] N. J. Mulgan and R. J. Ballagh, Phys. Rev. A **48**, 3321 (1993).
[4] G. Ankerhold, M. Schiffer, D. Mutschall, T. Scholz, and W. Lange, Phys. Rev. A **48**, R4031 (1993).
[5] M. Schiffer, G. Ankerhold, E. Cruse, and W. Lange, Phys. Rev. A **49**, R1558 (1994).
[6] M. Möller and W. Lange, Phys. Rev. A **49**, 4161 (1994).
[7] J. M. Williams and D. Williams, J. Opt. Soc. Am. **54**, 454 (1964).
[8] X. Ma and R. Lai, Phys. Rev. A **49**, 787 (1994).
[9] L. K. Lam, T. Fujimoto, and A. C. Gallagher, J. Chem. Phys. **68**, 3553 (1978).
[10] M. L. Yanson, V. B. Grushevskii, and Ya. Klyavinsh, Opt. Spectrosc. **67**, 305 (1989).
[11] J. Huennekens and A. Gallagher, Phys. Rev. A **28**, 238 (1983).
[12] M. G. Payne, J. E. Talmage, G. S. Hurst, and E. B. Wagner, Phys. Rev. A **9**, 1050 (1974).
[13] Z. Shippony and W. G. Read, J. Quant. Spectrosc. Radiat. Transfer **50**, 635 (1993).
[14] C. van Trigt, Phys. Rev. A **13**, 726 (1976).
[15] H. A. Post, Phys. Rev. A **33**, 2003 (1986).
[16] R. Lai, J. Chen, and X. Ma, Phys. Rev. A **50**, 3734 (1994).
[17] W. Falecki, W. Hartmann, and R. Boksch, Opt. Commun. **83**, 215 (1991).
[18] E. A. Milne, J. London Math. Soc. **1**, 40 (1926).
[19] T. Colbert and J. Huennekens, Phys. Rev. A **41**, 6145 (1990).
[20] G. J. Parker, W. N. Hitchon and J. E. Lawler, J. Phys. B **26**, 4643 (1993).
[21] T. Walker, D. Sesko, and C. Wieman, Phys. Rev. Lett. **64**, 408 (1990).
[22] R. Bonifacio and L. De Salvo, L. M. Narducci, and E. J. D'Angelo, Phys. Rev. A **50**, 1716 (1994).